PRELIMINARY RESULTS OF ATTENUATION ESTIMATION FROM TISSUE BACKSCATTER USING COMMERCIAL ULTRASONIC SCANNER

ZIEMOWIT KLIMONDA, JERZY LITNIEWSKI, ANDRZEJ NOWICKI

Institute of Fundamental Technical Research, Polish Academy of Sciences
Pawińskiego 5B, 02-106 Warsaw, Poland
zklim@ippt.gov.pl, jlitn@ippt.gov.pl,

Ultrasonography (USG) is a widespread and powerful tool used successfully in modern diagnostics. The standard USG scanner reflects impedance variations within the tissue that is penetrated by the ultrasound pulse. Although such image provides a lot of information to the physician, there are another parameters which could be imaged. The attenuation coefficient is one of them. Imaging of attenuation seems to be a promising tool for ultrasonic medical diagnostics. The attenuation estimation method based on the echoes mean frequency changes due to tissue attenuation dispersion is presented. The Doppler IQ technique is adopted to estimate the mean frequency changes directly from the raw RF data. The Singular Spectrum Analysis (SSA) technique is used for the mean frequency trend extraction. The changes of the mean frequency trend are related directly to the local attenuation coefficient. Preliminary results of the tissue phantom attenuation coefficient estimation and imaging using the commercial scanner are presented.

INTRODUCTION

The ultrasonic imaging is non-invasive, popular and relatively inexpensive method of visualization of the body interior. The basic operation principles of modern ultrasonic scanners remain unaltered from their origin. Short wideband pulse is transmitted by the transducer, that aperture determines the lateral resolution of the image. The pulse is transmitted through the tissue and the backscattered echoes are received. The envelope of the echo is subsequently detected and used to produce a single line of the ultrasonic image. Next, the aperture moves mechanically or electronically (in case of multi-element transducers) and the line forming process repeats. The image consists of many lines; each of them corresponds to the echo envelope. Such imaging mode is called B-mode (B comes from the brightness, since the amplitude of echoes is coded in a brightness scale and displayed

on a screen). The B-mode image reflects the distribution of the tissue reflectivity, that depends on acoustical impedance variations. However, the raw radio-frequency (RF) echoes contain information about the tissue properties that cannot be assessed with the signal envelope. The attenuation of ultrasound is one of such properties with potentially substantial importance in medical diagnostics. It has been demonstrated that pathological tissue differs in attenuating properties from the healthy one. Oosterveld et al. have shown that the slope of attenuation coefficient, combined with statistical parameters of image texture can be used to diagnose the diffuse liver disease [1]. Saijo et al. employed scanning acoustic microscope to measure five types of gastric cancer and indicated different attenuation coefficient and sound speed comparing to normal tissue [2]. Bigelow et al. investigated possibility of the prediction of the premature delivery based on the noninvasive ultrasonic attenuation determination [3]. In various other publications it has been reported that pathological processes can lead to changes in the mean attenuation coefficient that range from several percent for cirrhotic human liver, through dozens percent for fatty human liver [4], or degenerated bovine articular cartilage [5] to over a hundred percent in case of porcine liver HIFU treatment in vivo [6] or two hundred percent for porcine kidney thermal coagulation [7]. These reports motivated us to consider the parametric imaging of the attenuation as useful the tool in medical diagnostic. There are two approaches to the estimation of the ultrasonic attenuation. The spectral difference technique that is based on a comparison of the power spectrum of backscattered signals before and after the wave propagation through the medium and the spectral shift method that uses the downshift of the pulse mean frequency caused by the frequency-depended attenuation. In our approach the mean frequency (MF) is directly evaluated from the backscatter data by means of the correlation estimator. The details of this approach are described in "Methods section" of this paper. Mean frequency is highly variable due to the random character of the backscattering RF signals [8, 9]. In this work the Singular Spectrum Analysis (SSA) algorithm was used to extract the mean frequency trend and to minimize the random variance of the estimated attenuation profile. The data were collected from the tissue mimicking phantom using the commercial ultrasonic scanner equipped with the special research module capable to acquire RF data before envelope detection.

1. METHODS

We assumed, that the attenuation in tissue can be described by the following model. The amplitude of the wave propagating in tissue decreases exponentially due to attenuation what can be expressed as

$$A = A_0 \exp(-\alpha x) \tag{1}$$

where A_0 – initial intensity, α - attenuation coefficient and x – wave path length. The attenuation coefficient α depends on frequency f and in the soft tissue it has the following form:

$$\alpha(f) = \alpha_1 \left(\frac{f}{f_1} \right)^n \tag{2}$$

where α_1 is the attenuation coefficient at the frequency f_1 (in the literature generally f_1=*1 MHz*) and n for the soft tissue is close to 1 [10]. Thus, the linear relation between attenuation coefficient in tissue and the wave frequency is often assumed. When a short ultrasonic pulse propagates within the homogenous medium the dispersion of the attenuation

coefficient results in the shift of the pulse MF. To find estimates of the attenuation from ultrasonic echo signals we assume that the attenuation of tissue increases linearly with frequency and that the backscattered signals have the Gaussian shaped spectra (Gaussian pulses). Then, the MF shift (f-f_0) is given by [11, 12]

$$f - f_0 = \frac{\alpha \cdot \Delta x \cdot \sigma_0^{\,2}}{2} \tag{3}$$

where f_0 and f are MF before and after propagation respectively, σ_0^2 is the Gaussian variance of the pulse spectrum, Δx denotes penetrated distance and α is the attenuation coefficient. Gaussian pulse spectrum preserves the shape during propagation in linearly attenuating medium i.e. the σ_0^2 is constant, and the α can be calculated from the equation (3) as

$$\alpha = -\frac{2}{\sigma_0^{\,2}} \frac{\partial f}{\partial x} \tag{4}$$

The attenuation coefficient α is positive, thus MF along the propagation path i. e. the MF-line always decrease monotonically with the penetration depth.

To determine the MF-line we have applied the MF correlation estimator (I/Q algorithm). The estimator is defined by

$$MF = \frac{1}{2\pi T_s} a\tan\left(\frac{\sum_{i=1}^{N} Q(i)I(i+1) - Q(i+1)I(i)}{\sum_{i=1}^{N} I(i)I(i+1) + Q(i+1)Q(i)} \right) \tag{5}$$

where T_s is the sampling period and N is the estimator window length. The Q and I are quadrature and in-phase signal components. The N is very important parameter, because it is directly related to the resolution of the method. The Q and I are obtained by quadrature sampling technique. The quadrature sampling is often used in modern scanners and the correlation estimator is widely used in Doppler techniques [13].

The presented technique of attenuation estimation consists of four steps. First, the raw RF data (Fig. 1a) are filtered with the filter that bandwidth corresponds to the bandwidth of the transducer. Next the estimator window moves along the filtered RF-line and the MF values are determined. The MF- line is created point by point (Fig. 1b). In ideal case, the attenuation (A) line could be enumerated directly from MF-line using the eq. (4). Unfortunately, the real MF-lines are highly variable and the direct use of eq. (4) results with the highly noised A-lines, not suitable for the attenuation imaging. Thus, in the third step the reduction of the MF-line random variability is required. Two techniques are used. First, the moving average filter averaging over adjacent MF-lines in lateral direction is applied. Next the Singular Spectrum Analysis (SSA) trend extraction algorithm is used. The exemplary, smoothed MF-line is presented in Fig 1c.

The SSA is relatively new technique of analysis of the time series. The aim of this technique is the decomposition of the input data series into the sum of components which can be interpret as the trend, oscillatory components and the noise (non-oscillatory components). The major applications of the SSA technique is the smoothing of the time series, finding the trend, forecasting and detection of the structural changes [14-20] The SSA is the model-free technique - there is no need to know a general function describing how the MF changes with the depth. Another useful feature of the SSA is its robustness to the outliers [21].

The SSA is easy to use – it needs only one parameter – the window length. Details of this technique can be found in the literature [22].

The evaluation of the A-line from the extracted trend of MF-line by means of equation (4) is the last step of the presented attenuation estimation method. The coefficient in front of the derivative in the expression (4) can be found by the direct determination of σ_0^2 or by the measurement of the MF slope of the signal propagating in the tissue phantom with the known attenuation. The second approach was used in this paper. The exemplary A-line is presented in Fig 1d.

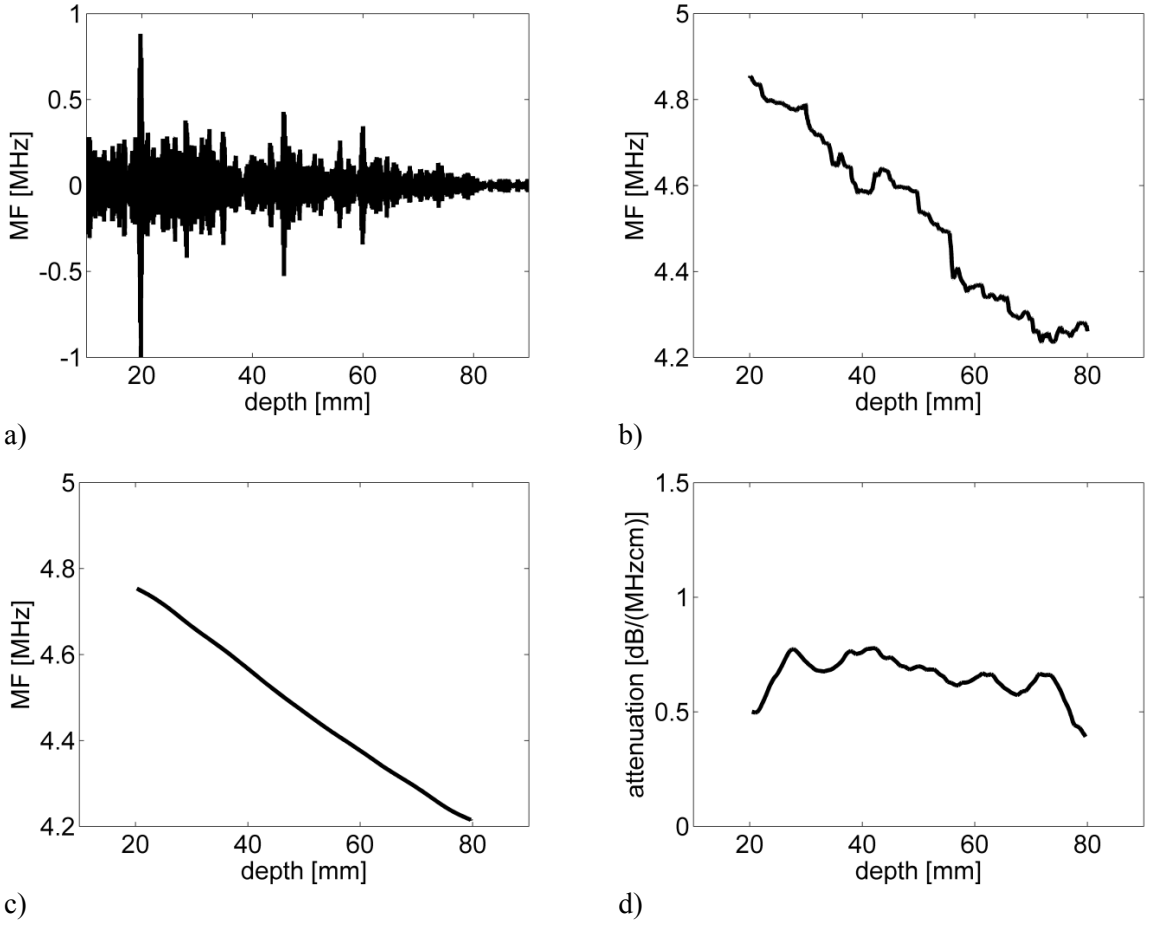

Fig.1. The example of RF-line (a), corresponding MF-line (b), averaged and SSA filtered MF-line (c) and the A-line (d). The correlation estimator window and the SSA algorithm window were equal to 2cm. The lateral averaging over 50 MF-lines was applied

2. EXPERIMENTAL SETUP

The experimental setup consisted of the tissue mimicking phantom produced by Dansk Fantom Design and the commercial ultrasonic scanner ZONARE z.one *ultra* SmartCart System. The attenuation of the phantom background was equaled 0.7 dB/MHzcm. It contained the cylindrical volume of the 1.5 cm diameter with the attenuation coefficient equal to 1.1 dB/(MHzcm). The cylinder was localized at 5 cm depth and its echogenicity was similar to the background echogenicity. The scanner was equipped with linear VF13-5 probe.

During imaging the scan plane was perpendicular to the cylinder axis. The pulse frequency was 5MHz. The scanner was equipped with the special research module (IQscan) that enables an access to the unprocessed RF data. The RF data were recorded during the scanning, transmitted to PC computer, and processed offline with the Matlab © software. The correlation estimator window length corresponded to 10 mm depth. Additionally, twelve RF scans of the phantom area with nominally uniform attenuation of 0.7 dB/(MHzcm) was recorded. This data were used to evaluate the coefficient $-2/\sigma_0^2$ of equation (4).

3. RESULTS

In Fig 3 the averaged MF-line and the equation used to fit linearly MF data is presented. The slope is equal to -0.1 while the phantom attenuation coefficient was equal to 0.7 dB/(MHzcm). That enables to determine $-2/\sigma_0^2$ coefficient from equation (4) that is equal to -7. This coefficient was used for the attenuation estimation from the data acquire from the cylinder.

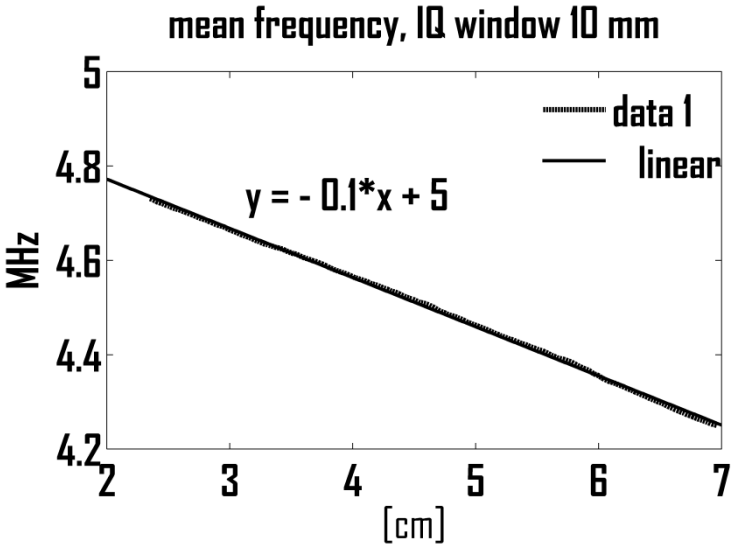

Fig.2. The mean frequency trend determined from the constant attenuation area of the tissue phantom

The results of a cylinder scan are presented in Fig 4. There is the B-mode image (a) of the cylinder and corresponding attenuation image (b). The cylinder is not well visible in B-mode image, because its echogenicity is similar to the background echogenicity. The cylinder is located approximately at 55 mm of y-axis and 25 mm of x-axis. The interior of the cylinder is slightly darker than the background. There is a dark "shadow" behind the cylinder. The shadow is visible because the ultrasounds passing the cylinder are more attenuated. The cylinder is well visible on attenuation image, however, its shape is distorted; it is not circular. The maximal value of the attenuation in the image is 1.4 dB/(MHzcm). The mean value of the attenuation of the object at the image depends on the size of the area used for averaging. For example, for an arbitrary chosen rectangle of the area of 8mm x 13mm (21-29mm x-axis and 52-65mm y-axis) what corresponds to the area of the highest brightness of the image, the mean attenuation equals to 1.1 dB/(MHzcm) what corresponds to the nominal attenuation of the cylinder. There are some variations of

the background attenuation. This "noise" could results from the inaccuracy of the method, or from the local heterogeneity of the phantom.

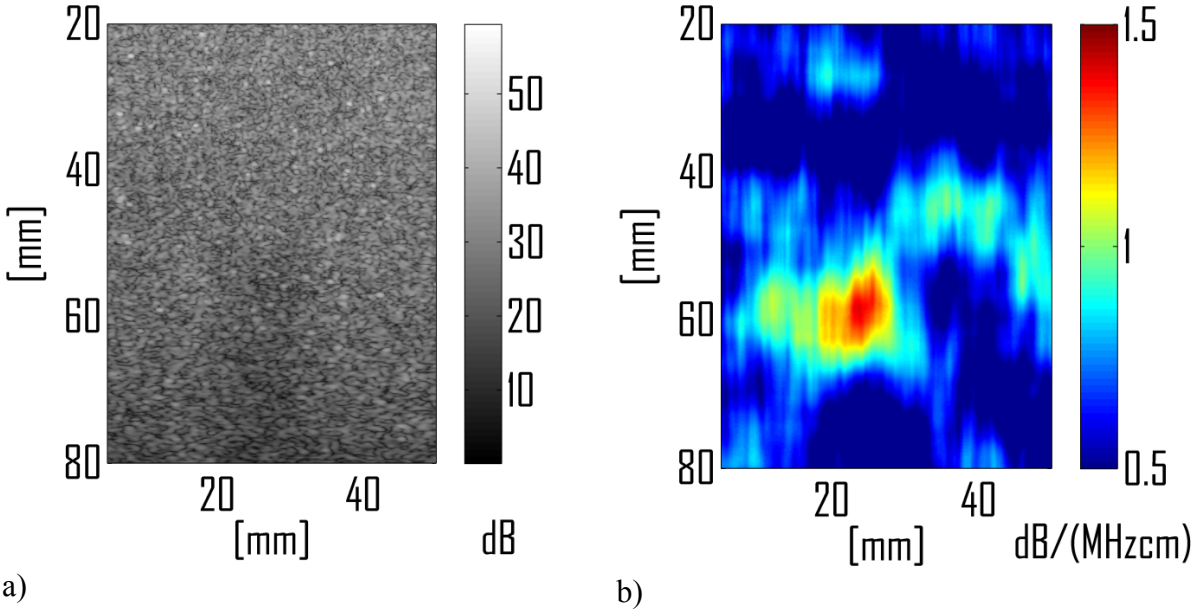

Fig.3. The acquired B-mode (a) and the corresponding local attenuation image

4. CONCLUSIONS

The method of parametric imaging of the tissue attenuation using commercial ultrasonic scanner is presented. It is based on measurements of the mean frequency changes of backscattered echoes received from the attenuating medium. The results proved that the method is capable to detect and to image the areas of different attenuation. The attenuation image visualize different attenuation properties of the tissue phantom better than the standard B-mode image. However, the attenuation image is distorted and noisy due to random character of the backscatter signals. The attenuation image presents different properties of a tissue comparing to traditional B-scan and despite poor resolution it provides additional information, potentially useful for the medical diagnostics.

Work supported in part by Ministry of Science and Higher Education, Poland (NN518388234).

REFERENCES

[1] B. J.Oosterveld, J.M. Thijssen, P.C. Hartman, R.L. Romijn, G. Josenbusch, Ultrasound attenuation and texture analysis of diffuse liver disease: methods and preliminary results, Phys. Med. Biol., Vol. 36(8), 1039–1064, 1991.

[2] Y. Saijo, High Frequency Acoustic Properties of Tumor Tissue. In: Ultrasonic Tissue Characterization, Springer-Verlag Tokio, 217-230, Hong-Kong 1996.

[3] T.A. Bigelow, B.L. Mcfarlin, W. D O'brien., M.L. Oelze, In vivo ultrasonic attenuation slope estimates for detectiong cervical ripening in rats: Preliminary results, Journal of Acoustical Society of America, Vol. 123(3), 1794-1800, 2008.

[4] Z.F. Lu, J. Zagzebski, F.T. Lee, Ultrasound Backscatter and Attenuation in Human Liver With Diffuse Disease, Ultrasound in Med. & Biol., Vol. 25(7), 1047-1054, 1999.

[5] H. J. Nieminen, S. Saarakkala, M.S. Laasanen, J. Hirvonen, J. S. Jurvelin, J. Töyräs Ultrasound Attenuation in Normal and Spontaneously Degenerated Articular Cartilage, Ultrasound in Med. & Biol., Vol. 30(4), 493-500, 2004.

[6] V. Zderic, A. Keshavarzi, A.M. Andrew, S. Vaezy, R.W. Martin, Attenuation of Porcine Tissues In Vivo After High Intensity Ultrasound Treatment, Ultrasound in Med. & Biol., Vol. 30(1), 61-66, 2004.

[7] A.E. Worthington, M.D. Sherar, Changes in Ultrasound Properties of Porcine Kidney Tissue During Heating, Ultrasound in Med. & Biol., Vol. 27(5), 673-682,2001.

[8] Z. Klimonda, A. Nowicki, Imaging of the mean frequency of the ultrasonic echoes, Archives of Acoustics, Vol. 32(4) (supplement), 77-80, 2007.

[9] J. Ophir, M.A. Ghouse, L.A. Ferrari, Attenuation estimation with the zero crossing technique: phantom studies, Ultras. Imag., Vol. 7, 122-132, 1985.

[10] A. Nowicki, Ultrasonic Diagnostics [in Polish: Diagnostyka Ultradźwiękowa], MAKmed, 2000c

[11] P. Laugier, G. Berger, M. Fink, J. Perrin, Specular reflector noise: effect and correction for in vivo attenuation estimation, Ultras. Imag. Vol. 7, 277-292, 1985.

[12] J. Litniewski, Assessment of trabecular bone structure deterioration by ultrasound [in Polish: Wykorzystanie fal ultradźwiękowych do oceny zmian struktury kości gąbczastej], Prace IPPT, 2006.

[13] A. Nowicki, Fundamentals of Doppler Ultrasonography [in Polish: Podstawy Ultrasonografii Dopplerowskiej], PWN, 1995.

[14] F. J. Alonso, J. M. Del Castillo, P. Pintado, Application of singular spectrum analysis to the smoothing of raw kinematic signals.,Journal of Biomechanics, Vol. 38, 1085-1092, 2005.

[15] N. E. Golyandina, K. D. Usevich, I. V. Florinsky, Filtering of Digital Terrain Models by Two-Dimensional Singular Spectrum Analysis, International Journal of Ecology & Development, Vol. 8(f07), 81-94, 2007.

[16] H.Hassani, Singular Spectrum Analysis: Methodology and Comparison, Journal of Data Science, Vol. 5, 239-257, 2007.

[17] J. C. Moore, A. Grinsted, Signular spectrum analysis and envelope detection: methods of enhancing the utility of ground-penetrating radar data, Journal of Glaciology, Vol. 52(176), 2006.

[18] D.H. Schoellhamer, Singular spectrum analysis for time series with missing data, Geophysical Research Letters, Vol. 28(16), 3187-3190, 2001.

[19] F. Varadi, R. K. Ulrich, L. Bertello, C. J. Henney, Random lag singular cross-spectrum analysis, The Astrophysical Journal, Vol. 528(1), 2000.

[20] R. Vautard, P. Yiou, M. Ghil, Singular-spectrum analysis: a toolkit for short, noisy chaotic signals, Physica D, Vol. 58, 95-126, 1992.
[21] T. Alexandrov, A Method of Trend Extraction using Singular Spectrum Analysis, REVSTAT Statistical Journal, Vol. 7(1), 1-22, 2009.
[22] N. Golyandina, V. Nekrutkin, A. Ahigljavsky, Analysis of time Series Structure: SSA and related techniques, Chapman & Hall/CRC, 2001.